



1 Iron-Bound Organic Carbon in Forest Soils: Quantification 2 and Characterization

3 Qian Zhao¹, Simon R Poulson², Daniel Obrist³, Samira Sumaila^{4, 5}, James J. Dynes⁴,
4 Joyce M. McBeth^{4, 5}, Yu Yang^{1*}

5 [1] {Department of Civil and Environmental Engineering, University of Nevada, Reno, Nevada, 89557}

6 [2] {Department of Geological Sciences and Engineering, University of Nevada, Reno, Nevada, 89557}

7 [3] {Division of Atmospheric Sciences, Desert Research Institute, Reno, Nevada, 89512}

8 [4] {Canadian Light Source, 44 Innovation Blvd, Saskatoon, SK, S7N 2V3, Canada}

9 [5] {Department of Geological Sciences, University of Saskatchewan, Saskatoon, SK, S7N 5E2, Canada}

10 * Correspondence to: Y. Yang (yuy@unr.edu)

11

12 ABSTRACT

13 Iron oxide minerals play an important role in stabilizing organic carbon (OC) and regulating the
14 biogeochemical cycles of OC on the earth surface. To predict the fate of OC, it is essential to
15 completely understand the amount, spatial variability and characteristics of Fe-bound OC in
16 natural soils. In this study, we investigated the concentrations and characteristics of Fe-bound OC
17 in soils collected from 14 forests in the United States, and determined the impact of
18 ecogeographical variables and soil physicochemical properties on the association of OC and Fe
19 minerals. We found that Fe-bound OC contributed up to 57.8% of total OC (TOC) in forest soils.
20 Atomic ratios of OC:Fe ranged from 0.56 to 17.7 with values of 1-10 for most samples, and these
21 ratios indicate an importance of both sorptive and incorporative interactions. The fraction of Fe-
22 bound OC in TOC ($f_{\text{Fe-OC}}$) was not related to the concentration of reactive Fe, which suggests that
23 the importance of association with Fe in OC accumulation was not governed by the concentration
24 of reactive Fe. Concentrations of Fe-bound OC and $f_{\text{Fe-OC}}$ increased with the latitude and reached
25 peak values at a site with a mean annual temperature of 6.6 °C. Attenuated total reflectance-Fourier
26 transform infrared spectroscopy (ATR-FTIR) and near-edge X-ray absorption fine structure
27 (NEXAFS) analyses revealed that Fe-bound OC was less aliphatic than non-Fe-bound OC. Fe-



28 bound OC also was more enriched in ^{13}C compared to the non-Fe-bound OC, but C/N ratios did
29 not differ substantially. In summary, ^{13}C -enriched OC with less aliphatic carbon and more
30 carboxylic carbon was associated with Fe minerals in the soils, with values of $f_{\text{Fe-OC}}$ being
31 controlled by both sorptive and incorporative associations between Fe and OC. Overall, this study
32 demonstrates that Fe oxides play an important role in regulating the biogeochemical cycles of C
33 in forest soils, and uncovers the governing factors for the spatial variability and characteristics of
34 Fe-bound OC.

35

36 1 Introduction

37 Soil organic carbon (OC) in forests contributes 40% of the global carbon (C) mass, and is
38 a vital component of C biogeochemical cycles (Eswaran et. al., 1999). Global warming can
39 potentially accelerate the decomposition of forest soil OC, contributing to greenhouse gas
40 emissions (Steffen et al., 1998). Alternatively, forest soils can act as strong sinks for OC, if
41 appropriate management is implemented, such as forest harvesting and fire treatment (Eswaran et.
42 al., 1999; Johnson and Curtis, 2001). Understanding the fate and stability of forest OC is important
43 for evaluating and managing the global C cycle under the framework of climate change.

44 Currently, there is a large information gap concerning the stability and residence time of
45 OC, contributing to the problem that the residence time of OC (ranging from months to hundreds
46 of years) is a major source of uncertainty in modeling and prediction of C cycles (Schmidt et al.,
47 2011; Riley et al., 2014). Many concepts have been proposed to account for OC stabilization and
48 therefore residence times, including molecular recalcitrance, physical occlusion, and chemical
49 protection (Sollins et al., 1996; Krull et al., 2003; Baldock et al., 2004; Mayer et al., 2004;
50 Zimmerman et al., 2004; Schmidt et al., 2011). In general, the stability of OC is regulated by
51 biogeochemical reactions occurring at the interfaces between OC, minerals, and microorganisms,
52 and further knowledge about the mechanism for OC stabilization is critical for building up process-
53 based models to simulate and predict C cycles.

54 A number of lines of evidence suggest a key importance of iron oxide minerals in the
55 stabilization of OC (Kalbitz et al., 2005; Kaiser and Guggenberger, 2007; Wagai and Mayer, 2007).
56 Iron oxides have a relatively high sorption capacity for OC, with sorption coefficients for OC much
57 higher than that of other metal oxides (Kaiser and Guggenberger, 2007; Chorover and Amistadi,



58 2001). Wagai and Mayer (2007) reported Fe-bound OC concentrations in soils up to 22 mg g⁻¹ soil,
59 contributing up to 40% of total OC (TOC) for most forest soils. Similarly, Lalonde et al. (2012)
60 found that Fe-bound OC contributed 22% of TOC in sediments. Studies have shown that Fe
61 minerals protect OC from degradation and inhibit mineralization of OC (Baldock and Skjemstad,
62 2000; Kalbitz et al., 2005). There is, however, no systematic study on the occurrence of Fe-bound
63 OC across different forests and its governing factors.

64 The overall goals of this study were to investigate the spatial variability of Fe-bound OC
65 across forest soils and the controlling factors, and to study the characteristics of Fe-bound OC in
66 respect to physicochemical properties of soils. In this study, we first quantified the concentration
67 of Fe-bound OC across 14 forest soils in the United States and analyzed the spatial distribution
68 and influences of ecogeographical factors. Second, we investigated the impact of soil
69 physicochemical properties on the Fe-OC associations. Third, we studied molecular characteristics
70 of Fe-bound OC versus non-Fe-bound OC, including how Fe-OC association influenced the
71 chemical properties of OC and their stable isotope composition. Hence, this study provided a
72 systematic evaluation for the Fe-bound OC in United States forests, the influences of ecological
73 factors on the occurrence of Fe-bound OC, and the effects of association with Fe on the chemical
74 properties of OC.

75

76 **2. Methods & Materials**

77 **2.1 Chemicals and materials**

78 Reagents used for Fe reduction experiments include sodium bicarbonate (NaHCO₃: Sigma-
79 Aldrich, St. Louis, MO, USA), trisodium citrate dihydrate (Na₃C₆H₅O₇•2H₂O: Acros Organics,
80 New Jersey, USA), and sodium dithionite (Na₂S₂O₄: Alfa Aesar, Ward Hill, MA, USA). All
81 chemicals used were analytical grade.

82

83 **2.2 Soil sample collection, primary characterization and pretreatment**

84 Soil samples were collected from 14 forest sites in the United States (Obrist et al., 2011,
85 2012, 2015). The abbreviations and the basic information for the sites are summarized in Table 1.
86 More detailed information on the sites and sampling protocols can be found in previous
87 publications (Obrist et al., 2011, 2012, 2015). Soil texture was analyzed by an ASTM 152-type



88 hydrometer at the Soil Forage and Water Analysis Laboratory at Oklahoma State University
89 (Obrist et al., 2011). The soil pH was measured by mixing soil particle with deionized (DI) water
90 in a solid/solution ratio of 1:1 (Kalra, 1995). Soil samples used in the experiments in this study
91 were ground to < 500 μm and freeze-dried.

92

93 **Table 1**

94

95 **2.3 Total C (TC), TOC and stable C isotope analyses**

96 TC, TOC and stable C isotopic compositions of soil samples were analyzed using a
97 Eurovector elemental analyzer (Eurovector SPA, Milan, Italy) interfaced to a Micromass IsoPrime
98 stable isotope ratio mass spectrometer (Micromass UK Ltd., Manchester, UK). Acetanilide (71.09 %
99 C by weight) was used as a standard compound to establish a calibration curve between mass of C
100 and the m/z 44 response from the mass spectrometer. In this study, the concentration of TC and
101 TOC were expressed as weight %. Stable C isotope analyses were performed after the method of
102 Werner et al. (1999), with results reported in the usual delta notation in units of ‰ vs. Vienna Pee
103 Dee Belemnite (VPDB). For TOC analysis, soil samples were acidified with 1 M HCl with the
104 solution/solid ratio of 1 mL solution/0.5 g soil and heated at 100°C for 1 hour. The treatment was
105 repeated three times until there was no further effervescence upon acid addition, after which the
106 samples were dried and analyzed.

107

108 **2.4 Nitrogen (N) analysis**

109 The N concentration of each sample was analyzed using a Eurovector elemental analyzer.
110 Acetanilide (10.36 % N by weight) was used as a standard compound to establish a calibration
111 curve between mass of N and the response of the thermal conductivity detector in the elemental
112 analyzer. Total N and non-Fe-bound N concentrations were measured before and after a Fe
113 reduction release treatment for each sample.

114

115 **2.5 Analysis of Fe-bound OC**

116 The concentration of Fe-bound OC was quantified by an established Fe reduction release
117 method, commonly known as DCB extraction involving sodium dithionite, citrate and bicarbonate
118 (Mehra and Jackson, 1960; Wagai and Mayer, 2007; Lalonde et al., 2012). The DCB extraction is



119 assumed to extract most free Fe oxides (i.e. goethite, hematite, ferrihydrite and others) existing in
120 soils, but should not extract structural Fe in clay minerals (Mehra and Jackson, 1960; Wagai and
121 Mayer et al., 2007; Lalonde et al., 2012). In this study, we followed the specific protocol detailed
122 in Lalonde et al. (2012). An aliquot (0.25 g) of soil was mixed with 15 mL of buffer solution at
123 pH 7 (containing 0.11 M bicarbonate and 0.27 M trisodium citrate), and then heated to 80°C in a
124 water bath. The reducing agent sodium dithionite was added to the samples with final
125 concentration of 0.1 M, and maintained at 80°C for 15 min. The samples were then centrifuged at
126 10,000 rpm for 10 min, the supernatant was removed, and the residual particles were rinsed using
127 5 mL of DI water. The rinse/centrifuge process was performed three times. The residual particles
128 were freeze-dried and analyzed for TC and TOC concentrations and $\delta^{13}\text{C}$ composition. The mass
129 of residual particles were used to calculate the OC concentration associated with non-Fe minerals.

130 The background release of OC during the heating process was measured following the
131 method in Lalonde et al. (2012), where sodium citrate and dithionite were replaced by sodium
132 chloride with the same ionic strength. An aliquot (0.25 g) of dry soil was mixed with 15 mL of 1.6
133 M NaCl and 0.11 M NaHCO_3 , and heated to 80°C. Then 0.22 g of NaCl was added, and the solution
134 was maintained at 80°C for 15 min. The samples were then centrifuged at 10,000 rpm and rinsed
135 three times, and freeze-dried before analysis. The mass of residual particles was used to calculate
136 the concentration of OC released by heating to 80°C. In preliminary experiments, we found that
137 the solution pH increased rapidly during the heating-extraction process with bicarbonate and
138 sodium chloride only, and the increased pH values facilitated the release of additional OC. Hence,
139 we used a lower initial pH of 6 to compensate for the shift to higher pH during heating. To validate
140 the measurement for the concentration of OC released during heating, we also tested the release of
141 OC using a phosphate buffer (same ionic strength) in lieu of the bicarbonate buffer, which can
142 maintain a pH of 7 during heating. Our results showed that the concentration of OC released was
143 similar for both the bicarbonate and phosphate buffer extraction reactions (Supplementary Material,
144 Fig. S1).

145

146 **2.6 Quantification of reactive Fe**

147 The concentration of reactive Fe in soils was determined by analyzing the Fe released
148 during the DCB reduction process. After the reduction treatment, the supernatant of each sample
149 was filtered using a 0.2 μm syringe filter (cellulose acetate), and analyzed for Fe concentration by



150 inductively coupled plasma - atomic emission spectroscopy (Varian-Vista AX CCD, Palo Alto,
151 CA, USA) at an optical absorption wavelength of 259.9 nm.

152

153 **2.7 Attenuated total reflectance-Fourier transform infrared spectroscopy (ATR-FTIR)**

154 ATR-FTIR analysis to characterize the molecular composition of OC was performed for
155 original soil samples and residual soils after DCB extraction using a Thermo Scientific Nicolet
156 6700 FTIR (Waltham, MA). Dry soil samples were placed directly on the crystal and forced to
157 contact well with the crystal. Spectra were acquired at the resolution of 4 cm^{-1} based on 100 scans.
158 Data collection and baseline correction were accomplished using OMNIC software version 8.3.103.

159

160 **2.8 Near-edge X-ray absorption fine structure (NEXAFS) analysis**

161 For further characterization of chemical structure of OM, carbon (1s) K-edge NEXAFS
162 analyses were performed for select soil samples, i.e. for soils with the highest and lowest values
163 of the fraction of Fe-bound OC to TOC. The soil particles were suspended in DI water and
164 deposited on an Au-coated silicon wafer attached to a Cu sample holder. Before analysis, samples
165 were dried in a vacuum desiccator. The X-ray-based experiments were performed on the Spherical
166 Grating Monochromator (SGM) beamline at the Canadian Light Source (Saskatoon, Canada)
167 (Regier et al., 2007). The energy scale was calibrated using citric acid (absorption at 288.6 eV).
168 Major technical parameters and set-up for the beamline include: X-ray energy ranges 250-2000
169 eV; 45 mm planer undulator; $1000\text{ }\mu\text{m}\times 100\text{ }\mu\text{m}$ spot size; silicon drift detectors (SDD); a titanium
170 filter before the sample; entrance and exit slit gaps of $249.9\text{ }\mu\text{m}$ and $25\text{ }\mu\text{m}$ (Gillespie et al., 2015).
171 Carbon 1s spectra were acquired by slew scans from 270 to 320 eV at 20 s dwell time and 20 scans
172 per sample on a new spot. For data normalization, I_0 was collected by measuring the scatter of the
173 incident beam from a freshly Au-coated Si wafer using SDD. Before the I_0 normalization, the pre-
174 edge baseline was adjusted to near zero to remove the scatter in the sample data (Gillespie et al.,
175 2015).

176 **3. Results and Discussion**

177 **3.1 Concentration of Fe-bound OC**

178 This study covered five major forest types in North America, including Spruce-Fir, Pine,
179 Oak, Chaparral, and Maple-beech-birch forests distributed between 29° and 47° N. For the 14



180 forest soils, TC concentrations ranged between 1.5 ± 0.1 and $8.3\pm 2.1\%$ (all percentages given are
181 weight-based), and TOC concentrations ranged between 1.3 ± 0.3 and $6.2\pm 2.9\%$, which are
182 comparable to values previously reported for North American forests (Wagai and Mayer, 2007;
183 Wilson et al., 2013). Bicarbonate extraction-calibrated Fe-bound OC concentrations ranged from
184 0.3 to 1.9%, with the fraction of Fe-bound OC to TOC ($f_{\text{Fe-OC}}$) averaging $37.8\pm 20.0\%$ (Fig. 1,
185 Supplementary Material, Table S1). Forest HL (Maine) had the highest $f_{\text{Fe-OC}}$ of 57.8%, while
186 forests GS (Florida) and OR (Tennessee) had $f_{\text{Fe-OC}}$ values below detection limits (i.e., below 0.6%).
187 Based on an estimate that 1502 Pg ($\text{Pg}=1\times 10^{15}$ g) of OC is stored in terrestrial soils (Scharlemann,
188 et al., 2014), scaling up these results to a global estimate would yield 538.5 ± 271.5 Pg of Fe-bound
189 OC residing in terrestrial soils. This is a very large pool, e.g. compared to an estimated 19-45 Pg
190 Fe-bound OC that reside in global surface marine sediments (Lalonde et al., 2012). As a major
191 component of the global C pool, Fe-bound OC in terrestrial soils therefore is expected to play a
192 key role in global C biogeochemical cycles.

193

194 **Fig. 1**

195

196 **3.2 Fe-OC association**

197 The values of $f_{\text{Fe-OC}}$ were influenced not only by the concentration of reactive Fe, but also
198 by the type of association between Fe and OC. In this study, the concentration of reactive Fe in
199 forest soils ranged from 0.1 mg g^{-1} to 19.3 mg g^{-1} , which is relatively low compared to values of
200 reactive Fe of up to 180 mg g^{-1} reported previously (Wagai and Mayer, 2007; Wagai et al., 2013)
201 (Fig. 2A). A Mollisol in forest sites MS (California) had the highest concentration of reactive Fe,
202 when a Spodosol in forest site GS (Florida) had the lowest reactive Fe concentration. To our
203 surprise, there was no significant correlation between $f_{\text{Fe-OC}}$ and the concentration of reactive Fe
204 (Pearson Correlation Coefficient $r=-0.418$, $p=0.137$, Fig. 2B). This suggests that the proportion of
205 Fe-bound OC is not strongly controlled by the reactive Fe concentration.

206 The OC:Fe molar ratio ranged from 0.56 to 17.7 for all 14 soils, with a value between 1
207 and 10 for 10 soils (Fig. 2A). Previous studies have suggested that the OC:Fe molar ratio can be
208 used as an indicator for the type of association between Fe oxides and OC, with lower values
209 indicating sorptive interactions, while higher values indicate incorporation of OC within Fe oxides
210 (Wagai et al., 2007; Guggenberger and Kaiser, 2003). The highest sorption capacity measured for



211 OC onto Fe oxide corresponds to an OC:Fe molar ratio = 1.0 (Kaiser and Guggenberger, 2006),
212 but by incorporation and co-precipitation of Fe oxide OC:Fe molar ratio can reach much higher
213 values (Guggenberger and Kaiser, 2003). With OC:Fe molar ratios generally between 1-10 for
214 most of the forest soils in this study, we propose that incorporation of OC into Fe oxides plays a
215 major role in the accumulation of Fe-bound OC exceeding sorption by at least a factor of 1 to 10
216 (Wagai and Mayer, 2007; Lalonde, 2012). However, for the HT (Michigan), HL (Maine) and TKF
217 (California) forest soils, the OC:Fe molar ratios were even higher than 10 with maximum value of
218 17.8 (Fig. 2A), implying that incorporation of OC into Fe oxides dominated at these sites. The
219 value of OC:Fe ratio was not related to the concentration of reactive Fe, and varied a lot for soils
220 with similar concentration of total reactive Fe (Fig. 2B). This indicates the type of interactions
221 between OC and Fe was not governed by the amount of Fe. The OC:Fe ratio is potentially regulated
222 by the mineral phases of Fe, as poorly-crystalline Fe oxide has a higher capacity to bind with OC
223 than crystalline Fe minerals (Eusterhues et al., 2014). When sorption dominates the interactions
224 between OC and Fe, OC:Fe can also be influenced greatly by the particle size and surface area of
225 Fe oxides (Gu et al., 1995). Further investigations are needed to determine the factors that control
226 the OC:Fe ratio, and also $f_{\text{Fe-OC}}$ values for soils. Nevertheless, the lack of (or poor) relationship
227 shown here between the concentration of Fe-bound OC and Fe concentrations demonstrates the
228 limitations associated with predicting and modeling the behavior of C in soils based on the Fe
229 concentrations in soils alone.

230

231 **Fig. 2.**

232

233 **3.3 Spatial variance and ecogeographical factors**

234 We analyzed the influences of ecogeographical factors on the occurrence of Fe-bound OC in forest
235 soils (Fig. 3). There was a significant correlation between the TOC concentration and latitude
236 (Pearson correlation coefficient $p=0.619$, $r=0.018$), a pattern commonly observed due to lower
237 microbial activity and turnover rates of C at higher, colder latitudes (Davidson and Janssens, 2006).
238 Concentration of reactive Fe, if excluding soil MS in California, it was also significantly related
239 to latitude ($p=0.824$, $r=0.001$). Both concentrations of Fe-bound OC and $f_{\text{Fe-OC}}$ also were correlated
240 with latitude ($p=0.523$, $r=0.053$; $p=0.525$, $r=0.054$). Among our samples, soil in forest HL in



241 Maine, one of the three northern-most site with latitude of 45° , had the highest $f_{\text{Fe-OC}}$ of 57.8%. In
242 forest GS in Florida with lowest latitude of 29.7° , the $f_{\text{Fe-OC}}$ were below detection limits, possibly
243 due to the low concentration of reactive Fe (0.08 mg g^{-1}). Hence, increase in latitude both increased
244 concentrations of TOC in soil as well concentrations of Fe-bound OC, suggesting increased
245 interactions between Fe oxide and OC at higher latitudes. There were no clear trends in TOC or
246 Fe-OC interactions with longitude. For elevation, we separated two groups of samples, with one
247 group located below 1000 m (asl) and the other group above (mainly around 2000 and 4000 asl).
248 Concentrations of TOC and Fe-bound OC, however, were not significantly different between the
249 two groups. There were no clear trends with precipitation either, although others have reported
250 positive relationships between mean annual precipitation and soil TOC concentration at a global
251 scale (Amundson, 2001). Both concentrations of Fe-bound OC and $f_{\text{Fe-OC}}$ reached highest value
252 with mean annual temperatures at 6.6°C . The increased annual mean temperature increased the
253 concentration of Fe-bound OC and $f_{\text{Fe-OC}}$ when it was below 6.6°C , then decreased when annual
254 mean temperature was over 6.6°C . Our results therefore suggest a possibly ideal temperature range
255 where Fe-OC interactions may be particularly pronounced. Finally, the study covered 7 major soil
256 orders, i.e. Alfisols (sample number $n=3$), Spodosols ($n=4$), Mollisols ($n=1$), Inceptisols ($n=2$),
257 Entisols ($n=2$), Gelisols ($n=1$), and Ultisols ($n=1$). Although there are limited replications in many
258 of these soil orders, highest concentration of Fe-bound OC were observed in Spodosols. Regarding
259 $f_{\text{Fe-OC}}$, the ratios also were highest in Spodosols, possibly indicating a particular importance of Fe-
260 bound OC in this soil type which occupies 3.5% of US land areas and 4% global ice-free land (Soil
261 Survey Staff, 1999). However, due to the limited number of samples for each soil order, these
262 findings warrant further confirmation.

263

264 **Fig. 3**

265

266 **3.4 Impact of soil physicochemical properties on Fe-OC association**

267

268 Soil texture can potentially influence the accumulation of Fe-bound OC. Figure 4
269 demonstrates that the fraction of non-calibrated Fe-bound OC showed a significant positive
270 correlation vs. fraction of sand ($r=0.72, p<0.001$), and negative correlations vs. fraction of silt ($r=-$
271 $0.697, p<0.001$) and fraction of clay ($r=-0.616, p<0.001$). There were similar correlations between



272 labile OC, and the fraction of sand ($r=0.72$, $p<0.001$), silt ($r=0.72$, $p<0.001$) and clay ($r=0.72$,
273 $p<0.001$). However, the calibrated Fe-bound OC had no significant correlation vs. any of the
274 texture fractions. These correlations indicate that the labile OC was mainly associated with the
275 sand component of forest soils, but that the soil texture did not affect the Fe-bound OC. There has
276 been debate on the relative roles of sand, clay and silt in the stabilization of OC in soil (Percival et
277 al., 2000; Six et al., 2002; Eusterhues et al., 2005; Vogel et al., 2014). Eusterhues et al. (2005)
278 found a relationship between the resistance of organic matter to oxidative degradation and the clay
279 concentration in soils, suggesting the importance of clay minerals in the stabilization and
280 accumulation of soil OC. In contrast, Percival et al. (2000) found that the clay mineral fraction
281 explained little of the variation in the accumulation of OC across a range of soil types in New
282 Zealand. Vogel et al. (2014) found that less than 20% of clay mineral surfaces were covered by
283 the sorption of OC, indicating that a limited proportion of clay mineral surface contributed towards
284 the stabilization of OC. Our results suggest that the Fe oxide-mediated stabilization of OC was not
285 related to the size/aggregation-based process, although the labile carbon concentrations increased
286 with the fraction of sand in the soils.

287

288 **Fig. 4**

289

290 The Fe-OC association can also be influenced by the soil pH, which affects the mineral
291 phases of Fe oxides and their surface charge, and their interactions with OC. For our soil samples,
292 the soil pH ranged from 4.1 to 6.3, similar to measurements by Wagai and Mayer (2007) for North
293 America soils. There was no significant correlation between the $f_{\text{Fe-OC}}$ and soil pH, e.g. the HL
294 (Maine) soil with pH of 4.4 had the highest $f_{\text{Fe-OC}}$ of 57.8%, while the TS(II) (Washington) soil
295 with a similar pH of 4.5 only had a $f_{\text{Fe-OC}}$ of 7.4%. For soils with pH ranging from 4.9 to 5.8, $f_{\text{Fe-OC}}$
296 did not change correspondingly. Contrastingly, values of OC:Fe molar ratios were significantly
297 influenced by the soil pH; expect for one outlier sample of TS(II) (Washington) soil, there was a
298 significant negative correlation between the OC:Fe molar ratio and soil pH ($r=-0.477$, $p=0.09$)
299 (Supplementary Material, Fig. S2). This may be due to the lower pH values favoring the
300 complexation and precipitation of Fe with OC, while higher pH favors sorptive interactions
301 between Fe minerals and OC (Tipping et al., 2002). If comparing samples with similar pH, the
302 soils with higher TOC had higher OC:Fe molar ratios, e.g. the GS soil (TOC = 1.1%) with pH of



303 4.7 had an OC:Fe molar ratio = 8.5, while the HT (Michigan) soil (TOC = 3.0%) with similar pH
304 of 4.7 had an OC:Fe molar ratio = 17.1. This was consistent with the concept model that the form
305 of Fe was dominated by the Fe-OC co-precipitated complex with relatively higher OC supply
306 (Schwertmann et al., 1986).

307

308 **3.5 Molecular characteristics of Fe-bound OC**

309 The chemical composition of Fe-bound OC can be substantially different from non-Fe-
310 bound OC (Adhikari and Yang, 2015) with broad implications on the C biogeochemical cycles,
311 although such differences so far have received limited attention. We analyzed the difference in
312 chemical composition of Fe-bound OC compared to non-Fe-bound OC using ATR-FTIR analysis
313 (Fig. 5). Overall, there were limited fingerprint peaks for OC, because of the low concentration of
314 TOC and technical challenge for analyzing whole soil particles with FTIR (Calderon et al., 2011;
315 Simonetti et al., 2012). Reeves (2012) demonstrated that FTIR analysis of mineral soils in the
316 ranges of 1600-1750 and 2800-3000 cm^{-1} only can be used to study OC. Peaks in the range of 500-
317 1200 cm^{-1} indicate the presence of clay or other Fe/Al minerals (Fig. 5) (Madejova, 2003; Harsh
318 et al., 2002; Parikh et al., 2014), such as kaolinite or montmorillonite at 850-1200 cm^{-1} (Madejova,
319 2003). Absorption at 850-1200 cm^{-1} can also be due to the presence of polysaccharides, but
320 definitive identification of polysaccharides is not possible in the presence of minerals (Senesi et
321 al., 2003; Tandy et al., 2010). The spectra in the range of 1600-1750 cm^{-1} normally contain
322 fingerprint peaks for functional groups of amides, carboxylates and aromatics (Parikh et al., 2014),
323 but we did not detect any significant peaks in this range. In the range of 2800-3000 cm^{-1} , there
324 were no significant peaks for the original soil samples, but after Fe extraction we detected
325 significant peaks at 2850 and 2930 cm^{-1} , which are characteristic for the presence of aliphatic
326 carbon. The substantial differences in spectra before and after Fe extraction indicate that aliphatic
327 OC was enriched in the residual soils after extraction. Other functional groups, such as aromatic
328 carbon and hydrophilic functional groups, were more strongly associated with Fe minerals and
329 removed during the Fe extraction, as hydrophilic functional groups can form inner-sphere
330 coordination complexation with iron oxides, and aromatic carbon has electron donor-acceptor
331 interactions with iron oxides (Gu et al., 1995; Axe and Persson, 2001).

332

333 **Fig. 5**



334

335 Furthermore, we analyzed the C 1s NEXAFS spectra of two original, non-extracted soils
 336 with the highest and lowest values of $f_{\text{Fe-OC}}$, i.e. HL (Maine) ($f_{\text{Fe-OC}}=57.8\%$) and OR (Tennessee)
 337 ($f_{\text{Fe-OC}}$ non-detectable) (Supplementary Material, Fig. S3). Three major fingerprint peaks were
 338 detected for both soils, including peaks at 285.3, 287.0 and 288.7 eV, which are corresponding to
 339 aromatic carbon, aliphatic carbon and carboxylic carbon, respectively (Schumacher et al., 2005;
 340 Solomon et al., 2005; Lehmann et al., 2008). The OR (Tennessee) soil had a more substantial
 341 signal at 287.0 eV than the HL (Maine) soil, indicating a higher aliphatic carbon concentration in
 342 the OR (Tennessee) soil compared to the HL (Maine) soil. Ratio of carboxylic carbon to aromatic
 343 carbon (peak height) was 3.8 for HL (Maine) and 1.0 for OR (Tennessee), suggesting that the HL
 344 (Maine) soil with higher $f_{\text{Fe-OC}}$ has relatively more carboxylic carbon compared to aromatic carbon.
 345 Hence, the C1s NEXAFS spectra suggest that the soil with the higher $f_{\text{Fe-OC}}$ has higher
 346 concentration of carboxylic C, while the soil with the lower $f_{\text{Fe-OC}}$ value has a higher aliphatic C
 347 concentration. This result is consistent with the comparison of ATR-FTIR spectra in soils before
 348 and after Fe extraction, providing evidence that Fe oxides are mainly associated with more
 349 hydrophilic and carboxylic carbon, while non-Fe-bound OC was more aliphatic.

350

351 To further investigate the relationships between soil OC and Fe minerals, we analyzed the
 352 stable C isotopic compositions ($\delta^{13}\text{C}$) of Fe-bound vs. non-Fe-bound OC (i.e., the residual OC
 353 after DCB extraction). The $\delta^{13}\text{C}$ for original soil samples ranged from -24.5% to -27.5% , and the
 354 values for non-Fe-bound OC were -25.1% to -28.0% . The $\delta^{13}\text{C}$ for Fe-bound OC was calculated
 355 by combined isotope-mass balance (equation (1))

$$356 \quad \delta^{13}\text{C}_{\text{TOC}} \times \text{TOC} = \delta^{13}\text{C}_{\text{labile}} \times \text{OC}_{\text{labile}} + \delta^{13}\text{C}'_{\text{Fe-OC}} \times \text{OC}'_{\text{Fe}} + \delta^{13}\text{C}_{\text{non-Fe-OC}} \times \text{OC}_{\text{non-Fe}} \quad (1)$$

357 where TOC is the concentration of total organic carbon, $\text{OC}_{\text{labile}}$ is the concentration of labile OC
 358 (extractable by bicarbonate buffer), $\text{OC}_{\text{non-Fe}}$ is the concentration of non-Fe-bound OC (residual
 359 OC after Fe extraction), and OC'_{Fe} is the concentration of Fe-bound OC (excluded the labile OC);
 360 $\delta^{13}\text{C}_{\text{TOC}}$ is $\delta^{13}\text{C}$ for bulk OC, $\delta^{13}\text{C}_{\text{labile}}$ is $\delta^{13}\text{C}$ for labile OC, $\delta^{13}\text{C}'_{\text{Fe-OC}}$ is $\delta^{13}\text{C}$ for Fe-bound OC,
 361 $\delta^{13}\text{C}_{\text{non-Fe-OC}}$ is $\delta^{13}\text{C}$ for non-Fe-bound OC. However, it is difficult to directly resolve the $\delta^{13}\text{C}_{\text{labile}}$
 362 and $\delta^{13}\text{C}'_{\text{Fe-OC}}$ using this equation. We simplified it to equation (2):

$$363 \quad \delta^{13}\text{C}'_{\text{Fe-OC}} = \frac{(\delta^{13}\text{C}_{\text{TOC}} \times \text{TOC} - \delta^{13}\text{C}_{\text{non-Fe-OC}} \times \text{OC}_{\text{non-Fe}})}{\text{OC}'_{\text{Fe}}} \quad (2)$$



364 where $\delta^{13}\text{C}_{\text{Fe-OC}}$ is $\delta^{13}\text{C}$ for Fe-bound OC (including the labile OC), $\delta^{13}\text{C}_{\text{TOC}}$ is $\delta^{13}\text{C}$ for bulk OC,
 365 $\delta^{13}\text{C}_{\text{non-Fe-OC}}$ is $\delta^{13}\text{C}$ for non-Fe-bound OC, TOC is the concentration of total organic carbon, $\text{OC}_{\text{non-}}$
 366 Fe is the concentration of non-Fe-bound OC, and OC_{Fe} is the concentration of Fe-bound OC. The
 367 $\delta^{13}\text{C}$ for Fe-bound OC was heaviest for the TKF (California) soil with a value of -23.0% , and the
 368 lightest for the GS (Florida) forest at -27.0% . Across all study sites, Fe-bound OC was relatively
 369 enriched in ^{13}C ($1.5\pm 1.2\%$ heavier) compared to the non-Fe-bound OC. However, there is also a
 370 contribution of labile OC to the Fe-bound OC, where labile OC is the OC extracted during the
 371 dithionite-absent extraction described earlier). The $\delta^{13}\text{C}$ value for labile OC can be calculated using
 372 equation (3):

$$373 \quad \delta^{13}\text{C}_{\text{labile}} = \frac{(\delta^{13}\text{C}_{\text{TOC}} \times \text{TOC} - \delta^{13}\text{C}_{\text{non-labile}} \times \text{OC}_{\text{non-labile}})}{\text{OC}_{\text{labile}}} \quad (3)$$

374 where $\delta^{13}\text{C}_{\text{labile}}$ is $\delta^{13}\text{C}$ for labile OC, $\delta^{13}\text{C}_{\text{TOC}}$ is $\delta^{13}\text{C}$ for bulk OC, $\delta^{13}\text{C}_{\text{non-labile}}$ is $\delta^{13}\text{C}$ for non-labile
 375 OC, $\text{OC}_{\text{non-labile}}$ is the concentration of non-labile OC, and $\text{OC}_{\text{labile}}$ is the concentration of labile OC.
 376 Calculated values of $\delta^{13}\text{C}_{\text{labile}}$ range from -23.4% to -30.3% , and were lighter than the values for
 377 $\delta^{13}\text{C}_{\text{Fe-OC}}$. Although it is not reliable to quantitatively calculate the $\delta^{13}\text{C}$ for Fe-bound OC
 378 subtracting the influences of labile OC, these results indicate that the true value for $\delta^{13}\text{C}_{\text{Fe-OC}}$ should
 379 be even somewhat heavier than the results presented in Fig. 6.

380 Our results demonstrate that Fe-bound OC was enriched in ^{13}C compared to the non-Fe-
 381 bound OC in forest soils, which is consistent with results for sediments, where Fe-bound OC was
 382 $1.7\pm 2.8\%$ heavier than non-Fe-bound OC (Lalonde et al., 2012) (Fig. 6A). Wang et al. (1998)
 383 have shown that ^{13}C -enriched organic matter in sediments was enriched with O and N (due to the
 384 presence of compounds such as proteins and carbohydrate groups), while the lipid fraction was
 385 relatively ^{13}C -depleted. Similarly, compound-specific isotopic analyses have shown that O/N-rich
 386 constituents, such as cellulose, hemi-cellulose and amino acids, are ^{13}C -enriched compared to
 387 hydrocarbons (Glaser, 2005), and these ^{13}C -enriched O/N-rich compounds can associate with Fe
 388 oxide extensively through inner-sphere coordination interactions (Parikh et al., 2014). The value
 389 of $\Delta^{13}\text{C}_{\text{FeOC-nonFeOC}}$ ($= \delta^{13}\text{C}_{\text{Fe-OC}} - \delta^{13}\text{C}_{\text{non-Fe-OC}}$) (difference in $\delta^{13}\text{C}$ for Fe-bound OC and non-Fe-
 390 bound OC) was inversely correlated with the molar ratio of OC:Fe ($r=-0.53$, $p=0.05$, Fig. 6B).
 391 These relationships suggest that the enrichment in ^{13}C was to some degree related to the OC:Fe
 392 ratio, with lower OC:Fe leading to higher enrichment in ^{13}C . As discussed previously, lower OC:Fe
 393 ratios indicate an increased contribution from sorptive interactions of OC with Fe minerals as
 394 compared to incorporation of OC within iron oxides and OC, and these sorptive interactions



395 between O/N-rich organic compounds and Fe oxide results in the enrichment of ^{13}C of Fe-bound
396 OC vs. non-Fe-bound OC. Previous studies have attributed the stability of relatively labile and
397 reactive compounds, such as amino acids and sugars, to their interactions with minerals (Schmidt
398 et al., 2011), and our results demonstrated the importance of sorption to Fe minerals in increasing
399 the stability of relatively reactive labile compounds.

400

401 **Fig. 6**

402

403 Nitrogen (N)-containing functional groups are potentially important for the association
404 between OC and Fe oxides, although the concentrations of N are much lower than C. The bulk soil
405 contained 0.05-0.45 % N, while the non-Fe-bound component (i.e. the residual solid after DCB
406 extraction) contained 0.06-0.32 % N. Concentrations of Fe-bound N, calculated by difference,
407 ranged up to 0.13 %. However, it is important to note that this number is based without a calibration
408 for labile N that may be removed by the dithionite-free DCB extraction (data not available). There
409 were significant correlations between C and N concentrations for both bulk soils ($r=0.847$, $p<0.001$:
410 Supplementary Material, Fig. S4) and the non-Fe-bound residual components ($r=0.858$, $p<0.001$:
411 Supplementary Material, Fig. S4), with molar C/N ratios of 14.2 ± 2.6 and 13.7 ± 2.3 for bulk and
412 non-Fe-bound OC, respectively. These C/N values are essentially identical to a previously
413 observed molar C/N ratio = 14.3 for a large set of world-wide soils samples (Cleveland et al.,
414 2007), and a molar C/N ratio = 14.4 for OC-rich samples in China (Tian et al., 2010). This result
415 suggests that C/N ratios for Fe-bound OC did not differ from that of non-Fe-bound OC, assuming
416 that the labile carbon did not have a substantially different C/N ratio. Therefore, in contrast to the
417 ^{13}C enrichment observed for Fe-bound OC, the interactions with Fe minerals did not affect the C/N
418 ratio substantially.

419

420 **4. Conclusion**

421 Fe oxides are recognized as an important mineral phase regulating the amount and characteristics
422 of OM in forest soils. The spatial variability of Fe-bound OC is governed by the geographical
423 factors, such as latitude and annual mean temperature, and also the soil physicochemical properties.



424 Chemical composition of Fe-bound OC is substantially different from the rest compartment of soil
425 OC. Overall, this study provided a comprehensive investigation into the spatial variance of Fe-
426 bound OC in forest soils, its governing factors, and how the Fe-OC associations affect the chemical
427 characteristics of OC. As a substantial amount of OC was bound to Fe oxides, and association with
428 Fe affected the quality of OC, Fe oxides can regulate the biogeochemical cycles of carbon and its
429 response to climate change.

430

431 **Acknowledgements**

432 This research was supported by DOE grant DE-SC0014275 and University of Nevada-Reno Start-
433 up Fund. NEXAF research described in this paper was performed at the Canadian Light Source,
434 which is supported by CFI, NSERC, the University of Saskatchewan, the Government of
435 Saskatchewan, WED Canada, NRC Canada, and CIHR. Sample collection was supported by a
436 former EPA Science-To-Achieve-Results (STAR) grant R833378. We also acknowledge the
437 helpful comments from the editor and reviewers during the stage of quick reports.

438

439 **References**

- 440 Adhikari, D. and Yang, Y.: Selective stabilization of aliphatic organic carbon by iron oxide, *Scientific*
441 *Reports*, 5, 2015.
- 442 Amundson, R.: The carbon budget in soils, *Annual Review of Earth and Planetary Sciences*, 29, 535-562,
443 2001.
- 444 Axe, K. and Persson, P.: Time-dependent surface speciation of oxalate at the water-boehmite (γ -
445 AlOOH) interface: Implications for dissolution, *Geochimica Et Cosmochimica Acta*, 65, 4481-4492, 2001.
- 446 Baldock, J. A. and Skjemstad, J. O.: Role of the soil matrix and minerals in protecting natural organic
447 materials against biological attack, *Organic Geochemistry*, 31, 697-710, 2000.
- 448 Baldock, J. A. and Skjemstad, J. O.: Role of the soil matrix and minerals in protecting natural organic
449 materials against biological attack, *Organic Geochemistry*, 31, 697-710, 2000.
- 450 Calderon, F. J., Reeves, J. B., III, Collins, H. P., and Paul, E. A.: Chemical Differences in Soil Organic
451 Matter Fractions Determined by Diffuse-Reflectance Mid-Infrared Spectroscopy, *Soil Science Society of*
452 *America Journal*, 75, 568-579, 2011.
- 453 Chorover, J. and Amistadi, M. K.: Reaction of forest floor organic matter at goethite, birnessite and smectite
454 surfaces, *Geochimica Et Cosmochimica Acta*, 65, 95-109, 2001.
- 455 Cleveland, C. C. and Liptzin, D.: C : N : P stoichiometry in soil: is there a "Redfield ratio" for the microbial
456 biomass?, *Biogeochemistry*, 85, 235-252, 2007.



- 457 Davidson, E. A. and Janssens, I. A.: Temperature sensitivity of soil carbon decomposition and feedbacks
458 to climate change, *Nature*, 440, 165-173, 2006.
- 459 Eswaran, H., Reich, P.F., Kimble, J.M., Beinroth, F.H., Padmanabhan, E., Moncharoen P: Global Climate
460 Change and Pedogenic Carbonates. Lal, R. (Ed.), Lewis Publishers, 1999.
- 461 Eusterhues, K., Hadrich, A., Neidhardt, J., Kusel, K., Keller, T. F., Jandt, K. D., and Totsche, K. U.:
462 Reduction of ferrihydrite with adsorbed and coprecipitated organic matter: microbial reduction by
463 *Geobacter bremerensis* vs. abiotic reduction by Na-dithionite, *Biogeosciences*, 11, 4953-4966, 2014.
- 464 Eusterhues, K., Rumpel, C., and Kogel-Knabner, I.: Organo-mineral associations in sandy acid forest soils:
465 importance of specific surface area, iron oxides and micropores, *European Journal of Soil Science*, 56, 753-
466 763, 2005.
- 467 Gillespie, A. W., Phillips, C. L., Dynes, J. J., Chevrier, D., Regier, T. Z., and Peak, D.: Advances in Using
468 Soft X-Ray Spectroscopy for Measurement of Soil Biogeochemical Processes, *Advances in Agronomy*,
469 Vol 133, 133, 1-32, 2015.
- 470 Glaser, B.: Compound-specific stable-isotope (δ C-13) analysis in soil science, *Journal of Plant*
471 *Nutrition and Soil Science*, 168, 633-648, 2005.
- 472 Gu, B. H., Schmitt, J., Chen, Z., Liang, L. Y., and McCarthy, J. F.: ADSORPTION AND DESORPTION
473 OF DIFFERENT ORGANIC-MATTER FRACTIONS ON IRON-OXIDE, *Geochimica Et Cosmochimica*
474 *Acta*, 59, 219-229, 1995.
- 475 Guggenberger, G. and Kaiser, K.: Dissolved organic matter in soil: challenging the paradigm of sorptive
476 preservation, *Geoderma*, 113, 293-310, 2003.
- 477 Harsh, J. B., Chorover, J., Nizeyimana, E.: Allophane and imogolite. Chap. 9. In: *Soil Mineralogy with*
478 *environmental applications*, Dixon, J. B., Schulze, D. G.: (Ed.), Book Series SSSA No. 7, Madison, WI,
479 2002.
- 480 Johnson, D. W., and Curtis, P. S.: Effects of forest management on soil C and N storage: meta analysis.
481 *Forest Ecology and Management*, 140, 227-238, 2001.
- 482 Kaiser, K. and Guggenberger, G.: Sorptive stabilization of organic matter by microporous goethite: sorption
483 into small pores vs. surface complexation, *European Journal of Soil Science*, 58, 45-59, 2007.
- 484 Kalbitz, K., Schwesig, D., Rethemeyer, J., and Matzner, E.: Stabilization of dissolved organic matter by
485 sorption to the mineral soil, *Soil Biology & Biochemistry*, 37, 1319-1331, 2005.
- 486 Kalra, Y. P., Agrawal, H. P., Allen, E., Ashworth, J., Audesse, P., Case, V. W., Collins, D., Combs, S. M.,
487 Dawson, C., Denning, J., Donohue, S. J., Douglas, B., Drought, B. G., Flock, M. A., Friedericks, J. B.,
488 Gascho, G. J., Gerstl, Z., Hodgins, L., Hopkins, B., Horneck, D., Isaac, R. A., Kelly, P. M., Konwicki, J.,
489 Kovar, J., Kowalenko, G., Lutwick, G., Miller, R. O., Munter, R., Murchison, I., Neary, A., Neumann, R.,
490 Neville, M., Nolan, C. B., Olive, R., Pask, W., Pastorek, L., Peck, T. R., Peel, T., Ramakers, J., Reid, W.
491 S., Rodd, V., Schultz, R., Simard, R., Singh, R. S., Sorrels, J., Sullivan, M., Tran, S., Trenholm, D., Trush,
492 J., Tucker, M. R., Turcotte, E., Vannierkerk, A., Vijan, P. N., Villanueva, J., Wang, C., Warncke, D. D.,
493 Watson, M. E., Wikoff, L., and Yeung, P.: DETERMINATION OF PH OF SOILS BY DIFFERENT
494 METHODS - COLLABORATIVE STUDY, *Journal of Aoac International*, 78, 310-324, 1995.



- 495 Krull, E. S., Baldock, J. A., and Skjemstad, J. O.: Importance of mechanisms and processes of the
496 stabilisation of soil organic matter for modelling carbon turnover, *Functional Plant Biology*, 30, 207-222,
497 2003.
- 498 Lalonde, K., Mucci, A., Ouellet, A., and Gelinas, Y.: Preservation of organic matter in sediments promoted
499 by iron, *Nature*, 483, 198-200, 2012.
- 500 Lehmann, J., Solomon, D., Kinyangi, J., Dathe, L., Wirrick, S., and Jacobsen, C.: Spatial complexity of soil
501 organic matter forms at nanometre scales, *Nature Geoscience*, 1, 238-242, 2008.
- 502 Madejova, J.: FTIR techniques in clay mineral studies, *Vibrational Spectroscopy*, 31, 1-10, 2003.
- 503 Mayer, L. M., Schick, L. L., Hardy, K. R., Wagai, R., and McCarthy, J.: Organic matter in small mesopores
504 in sediments and soils, *Geochimica Et Cosmochimica Acta*, 68, 3863-3872, 2004.
- 505 Mehra, O. P., and Jackson, M. L.: Iron oxide removal from soils and clays by a dithionite-citrate system
506 buffered with sodium bicarbonate, In *National Conference on Clays and Clay minerals*, 7, 317-327, 1960.
- 507 Obrist, D.: Mercury Distribution across 14 U.S. Forests. Part II: Patterns of Methyl Mercury Concentrations
508 and Areal Mass of Total and Methyl Mercury, *Environmental Science & Technology*, 46, 5921-5930, 2012.
- 509 Obrist, D., Johnson, D. W., Lindberg, S. E., Luo, Y., Hararuk, O., Bracho, R., Battles, J. J., Dail, D. B.,
510 Edmonds, R. L., Monson, R. K., Ollinger, S. V., Pallardy, S. G., Pregitzer, K. S., and Todd, D. E.: Mercury
511 Distribution Across 14 US Forests. Part I: Spatial Patterns of Concentrations in Biomass, Litter, and Soils,
512 *Environmental Science & Technology*, 45, 3974-3981, 2011.
- 513 Obrist, D., Zielinska, B., and Perlinger, J. A.: Accumulation of polycyclic aromatic hydrocarbons (PAHs)
514 and oxygenated PAHs (OPAHs) in organic and mineral soil horizons from four US remote forests,
515 *Chemosphere*, 134, 98-105, 2015.
- 516 Parikh, S. J., Goyné, K. W., Margenot, A. J., Mukome, F. N. D., and Calderon, F. J.: Soil Chemical Insights
517 Provided through Vibrational Spectroscopy, *Advances in Agronomy*, Vol 126, 126, 1-148, 2014.
- 518 Percival, H. J., Parfitt, R. L., and Scott, N. A.: Factors controlling soil carbon levels in New Zealand
519 grasslands: Is clay content important?, *Soil Science Society of America Journal*, 64, 1623-1630, 2000.
- 520 Reeves, J. B., III: Mid-infrared spectral interpretation of soils: Is it practical or accurate?, *Geoderma*, 189,
521 508-513, 2012.
- 522 Regier, T., Krochak, J., Sham, T. K., Hu, Y. F., Thompson, J., and Blyth, R. I. R.: Performance and
523 capabilities of the Canadian Dragon: The SGM beamline at the Canadian Light Source, *Nuclear Instruments
524 & Methods in Physics Research Section a-Accelerators Spectrometers Detectors and Associated Equipment*,
525 582, 93-95, 2007.
- 526 Riley, W. J., Maggi, F., Kleber, M., Torn, M. S., Tang, J. Y., Dwivedi, D., and Guerry, N.: Long residence
527 times of rapidly decomposable soil organic matter: application of a multi-phase, multi-component, and
528 vertically resolved model (BAMS1) to soil carbon dynamics, *Geoscientific Model Development*, 7, 1335-
529 1355, 2014.
- 530 Scharlemann, J. P. W., Tanner, E. V. J., Hiederer, R., and Kapos, V.: Global soil carbon: understanding and
531 managing the largest terrestrial carbon pool, *Carbon Management*, 5, 81-91, 2014.



- 532 Schmidt, M. W. I., Torn, M. S., Abiven, S., Dittmar, T., Guggenberger, G., Janssens, I. A., Kleber, M.,
 533 Kogel-Knabner, I., Lehmann, J., Manning, D. A. C., Nannipieri, P., Rasse, D. P., Weiner, S., and Trumbore,
 534 S. E.: Persistence of soil organic matter as an ecosystem property, *Nature*, 478, 49-56, 2011.
- 535 Schumacher, M., Christl, I., Scheinost, A. C., Jacobsen, C., and Kretzschmar, R.: Chemical heterogeneity
 536 of organic soil colloids investigated by scanning transmission X-ray microscopy and C-1s NEXAFS
 537 microspectroscopy, *Environmental Science & Technology*, 39, 9094-9100, 2005.
- 538 Schwertmann, U. and Latham, M.: PROPERTIES OF IRON-OXIDES IN SOME NEW CALEDONIAN
 539 OXISOLS, *Geoderma*, 39, 105-123, 1986.
- 540 Senesi, N., D'Orazio, V., and Ricca, G.: Humic acids in the first generation of EUROSOLS, *Geoderma*,
 541 116, 325-344, 2003.
- 542 Simonetti, G., Francioso, O., Nardi, S., Berti, A., Brugnoli, E., Lugato, E., and Morari, F.: Characterization
 543 of Humic Carbon in Soil Aggregates in a Long-term Experiment with Manure and Mineral Fertilization,
 544 *Soil Science Society of America Journal*, 76, 880-890, 2012.
- 545 Six, J., Callewaert, P., Lenders, S., De Gryze, S., Morris, S. J., Gregorich, E. G., Paul, E. A., and Paustian,
 546 K.: Measuring and understanding carbon storage in afforested soils by physical fractionation, *Soil Science
 547 Society of America Journal*, 66, 1981-1987, 2002.
- 548 Sollins, P., Homann, P., and Caldwell, B. A.: Stabilization and destabilization of soil organic matter:
 549 Mechanisms and controls, *Geoderma*, 74, 65-105, 1996.
- 550 Solomon, D., Lehmann, J., Kinyangi, J., Liang, B. Q., and Schafer, T.: Carbon K-edge NEXAFS and FTIR-
 551 ATR spectroscopic investigation of organic carbon speciation in soils, *Soil Science Society of America
 552 Journal*, 69, 107-119, 2005.
- 553 Staff, S. S.: Soil taxonomy: A basic system of soil classification for making and interpreting soil surveys.
 554 2nd edition, Natural Resources Conservation Service. U.S. Department of Agriculture Handbook 436, 1999.
- 555 Steffen, W., Noble, I., Canadell, J., Apps, M., Schulze, E. D., Jarvis, P. G., Baldocchi, D., Ciais, P., Cramer,
 556 W., Ehleringer, J., Farquhar, G., Field, C. B., Ghazi, A., Gifford, R., Heimann, M., Houghton, R., Kabat,
 557 P., Korner, C., Lambin, E., Linder, S., Mooney, H. A., Murdiyarso, D., Post, W. M., Prentice, I. C., Raupach,
 558 M. R., Schimel, D. S., Shvidenko, A., Valentini, R., and Terrestrial Carbon Working, G.: The terrestrial
 559 carbon cycle: Implications for the Kyoto Protocol, *Science*, 280, 1393-1394, 1998.
- 560 Tandy, S., Healey, J. R., Nason, M. A., Williamson, J. C., Jones, D. L., and Thain, S. C.: FT-IR as an
 561 alternative method for measuring chemical properties during composting, *Bioresource Technology*, 101,
 562 5431-5436, 2010.
- 563 Tian, H., Chen, G., Zhang, C., Melillo, J. M., and Hall, C. A. S.: Pattern and variation of C:N:P ratios in
 564 China's soils: a synthesis of observational data, *Biogeochemistry*, 98, 139-151, 2010.
- 565 Tipping, E., Rey-Castro, C., Bryan, S. E., and Hamilton-Taylor, J.: Al(III) and Fe(III) binding by humic
 566 substances in freshwaters, and implications for trace metal speciation, *Geochimica Et Cosmochimica Acta*,
 567 66, 3211-3224, 2002.
- 568 Vogel, C., Mueller, C. W., Hoeschen, C., Buegger, F., Heister, K., Schulz, S., Schloter, M., and Koegel-
 569 Knabner, I.: Submicron structures provide preferential spots for carbon and nitrogen sequestration in soils,
 570 *Nature Communications*, 5, 2014.



571 Wagai, R. and Mayer, L. M.: Sorptive stabilization of organic matter in soils by hydrous iron oxides,
572 *Geochimica Et Cosmochimica Acta*, 71, 25-35, 2007.

573 Wagai, R., Mayer, L. M., Kitayama, K., and Shirato, Y.: Association of organic matter with iron and
574 aluminum across a range of soils determined via selective dissolution techniques coupled with dissolved
575 nitrogen analysis, *Biogeochemistry*, 112, 95-109, 2013.

576 Wang, X. C., Druffel, E. R. M., Griffin, S., Lee, C., and Kashgarian, M.: Radiocarbon studies of organic
577 compound classes in plankton and sediment of the northeastern Pacific Ocean, *Geochimica Et*
578 *Cosmochimica Acta*, 62, 1365-1378, 1998.

579 Werner, R. A., Bruch, B. A., and Brand, W. A.: ConFlo III - An interface for high precision delta(13)C and
580 delta(15)N analysis with an extended dynamic range, *Rapid Communications in Mass Spectrometry*, 13,
581 1237-1241, 1999.

582 Wilson, B. T., Woodall, C.W., and Griffith, D.M. : Imputing forest carbon stock estimates from inventory
583 plots to a nationally continuous coverage, *Carbon Balance and Management*, 8, 2013.

584

585

586

587

588

589

590

591

592

593

594

595

596

597

598

599

600

601

602

603

604



605 **Figure Captions**

606 **Figure 1.** Concentrations of total carbon (TC), total organic carbon (TOC) and Fe-bound OC in
607 14 forest soils across the United States. Duplicate measurements were conducted for each of two
608 plots in every forest site. Error bars represent standard deviation of measurements of four replicates
609 for each forest site.

610 **Figure 2. A** Concentration of reactive Fe and OC:Fe molar ratio in US forest soils. **B** Relationship
611 between the fraction of Fe-bound OC in TOC ($f_{\text{Fe-OC}}$)/ OC:Fe molar ratio and reactive Fe
612 concentration in US forest soils.

613 **Figure 3.** Correlation between the TOC, reactive Fe, concentration of Fe-bound OC, $f_{\text{Fe-TOC}}$, OC:Fe
614 and ecogeographical parameters including latitude, longitude, elevation (asl), precipitation (mean
615 annual) and temperature (annual mean).

616 **Figure 4.** Correlation of the fractions of iron-bound organic carbon (uncalibrated and calibrated
617 for loss of labile OC) and labile organic carbon vs. fractions of sand, silt, and clay in forest soils.

618 **Figure 5.** Attenuated total reflectance-Fourier transform infrared spectroscopy (ATR-FTIR)
619 analysis for representative forest soils before (black line) and after Fe extraction (red line). All the
620 spectra are background-calibrated. Among the 14 forest soils sampled in this study, we used five
621 different forest soils, with $f_{\text{Fe-OC}}$ ranging 5.6-57.8%.

622 **Figure 6. A.** $\delta^{13}\text{C}$ of total organic carbon and non-iron bound organic carbon for 14 U.S. forest
623 sites. **B.** Correlation between $\Delta^{13}\text{C}_{\text{FeOC-nonFeOC}}$ and molar ratio of OC:Fe.

624

625

626

627

**Table 1 Information for the 14 forest sites studied (Obrist et al., 2011, 2012, 2015)**

Forest ID	Abb. r.	Location	Soil Order	Climate Zone	Precip. ^a (mm y ⁻¹)	Temp ^b (°C)	LAT(°) c	LONG(°) d	Elevation (m asl)
Ashland	AL	Ashland, Missouri	Alfisols	Humid Continental	1023	13.9	38.73	-92.20	210
Bartlett	BL	Bartlett, New Hampshire	Spodosols	Humid Continental	1300	4.5	44.0	-71.29	272
Marysville	MS	Marysville, California	Mollisols	Mediterranean climate	775	16.9	39.25	-121.28	386
Gainesville	GS	Gainesville, Florida	Spodosols	Humid Subtropical	1228	21.7	29.74	-82.22	50
Oak Ridge	OR	Oak Ridge, Tennessee	Ultisols	Humid Subtropical	1350	14.5	35.97	-84.28	
Little Valley (post-fire)	LV F	Little Valley, Nevada	Entisols	Highland Climate	551	5.0	39.12	-119.93	2010
Little Valley	LV	Little Valley, Nevada	Entisols	Highland Climate	550	5.0	39.12	-119.93	2011
Truckee (post-fire)	TK F	Truckee, California	Alfisols	Highland Climate	569	6.0	39.37	-120.1	1768
Truckee	TK	Truckee, California	Alfisols	Highland Climate	568	5.9	39.37	-120.1	1767
Niwot Ridge	NR	Niwot Ridge, Colorado	Alfisols	Highland Climate	800	1.3	40.03	-105.55	3050
Hart	HT	Hart, Michigan	Spodosols	Humid Continental	812	7.6	43.67	-86.15	210
Howland	HL	Howland, Maine	Spodosols	Humid Continental	1040	6.7	45.20	-68.74	60
Thompson I	TSI	Ravensdale, Washington	Inceptisols	Highland Climate	1141	9.8	47.38	-121.93	221
Thompson II	TSI I	Ravensdale, Washington	Inceptisols	Highland Climate	1140	9.8	47.38	-121.93	220

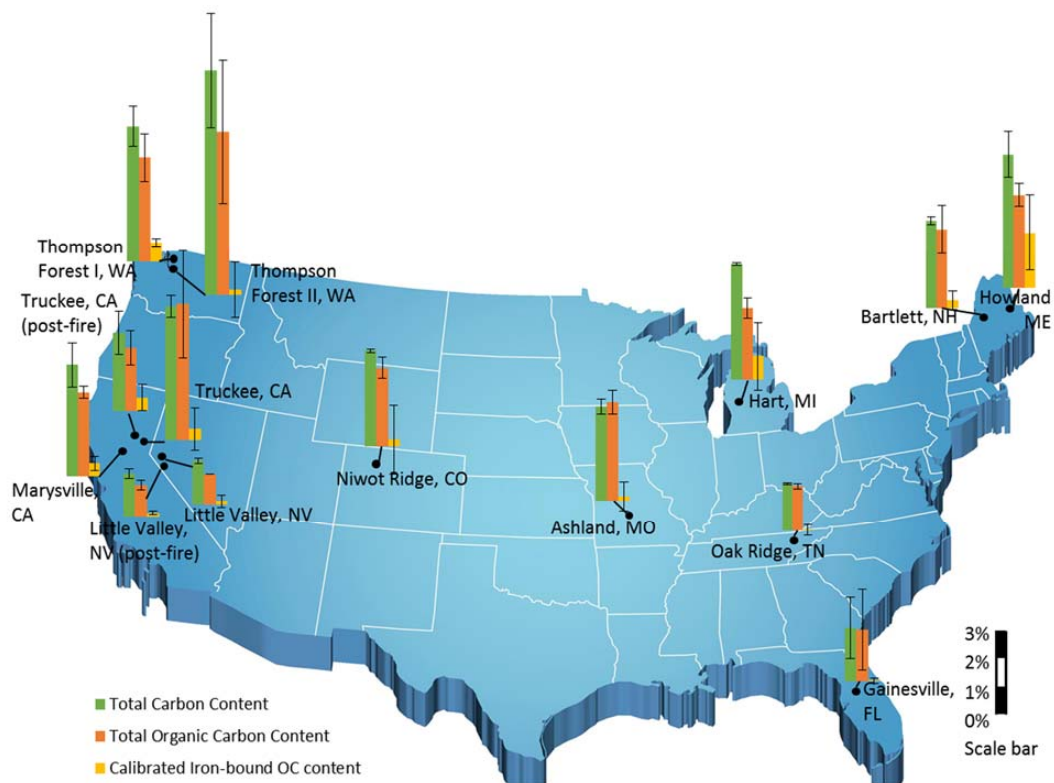
a: annual precipitation; b: annual mean temperature; c latitude; d: longitude.

628

629

630

631



632

633 **Fig. 1**

634

635

636

637

638

639

640

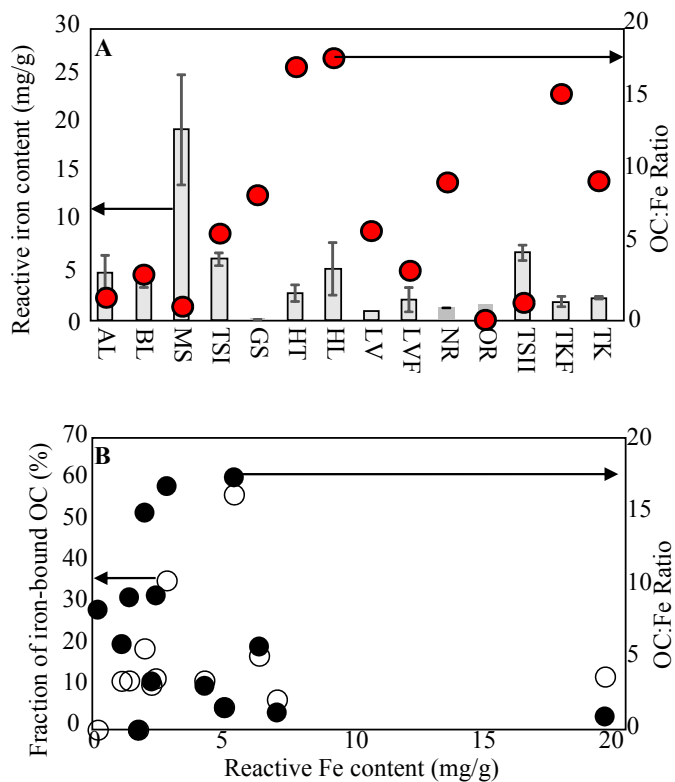
641

642

643

644

645



646

647 **Fig. 2**

648

649

650

651

652

653

654

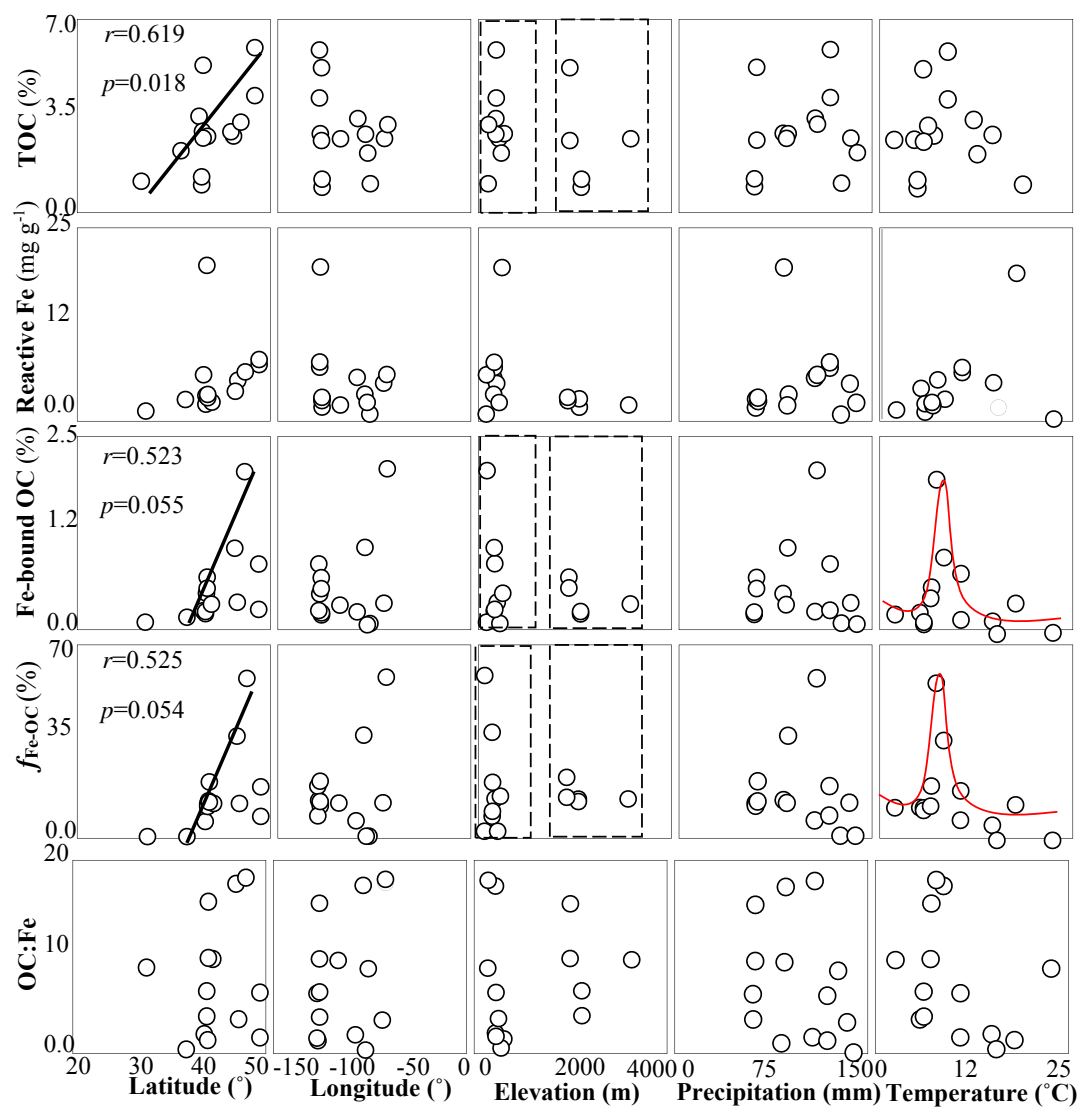
655

656

657

658

659



660

661 **Fig. 3**

662

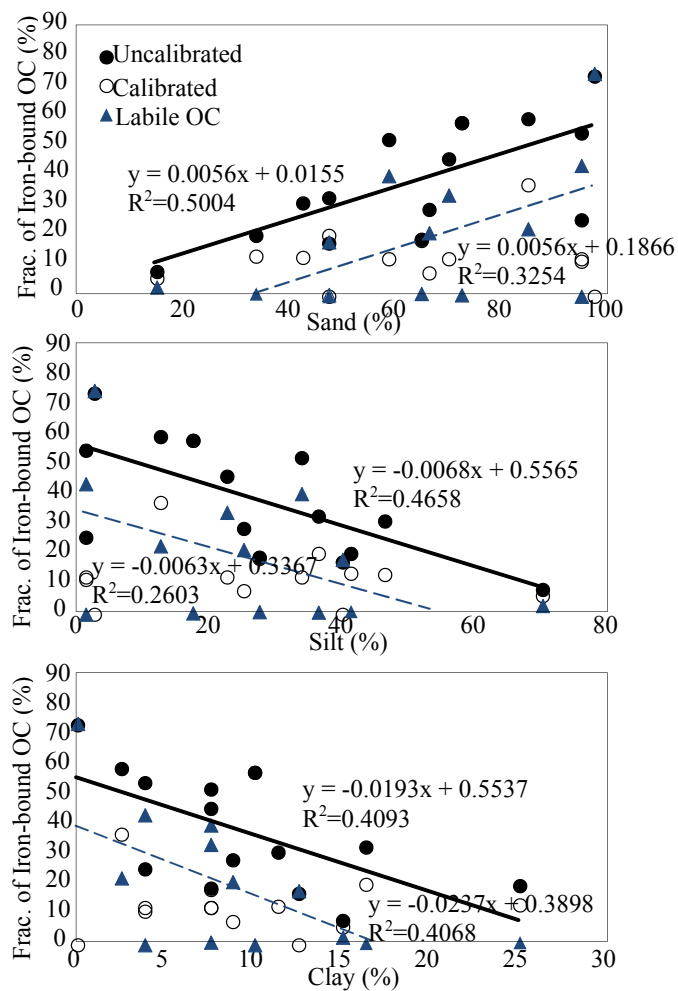
663

664

665

666

667



668

669 **Fig. 4**

670

671

672

673

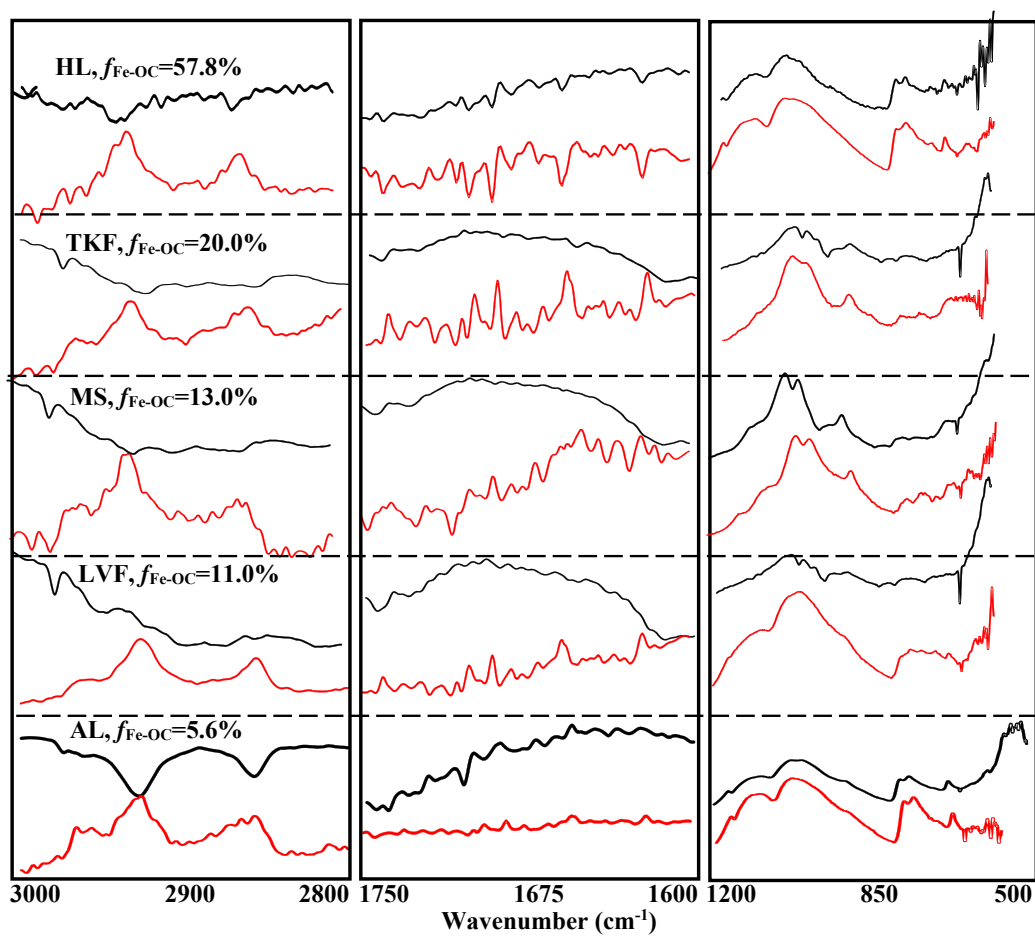
674

675

676

677

678



679

680 **Fig. 5**

681

682

683

684

685

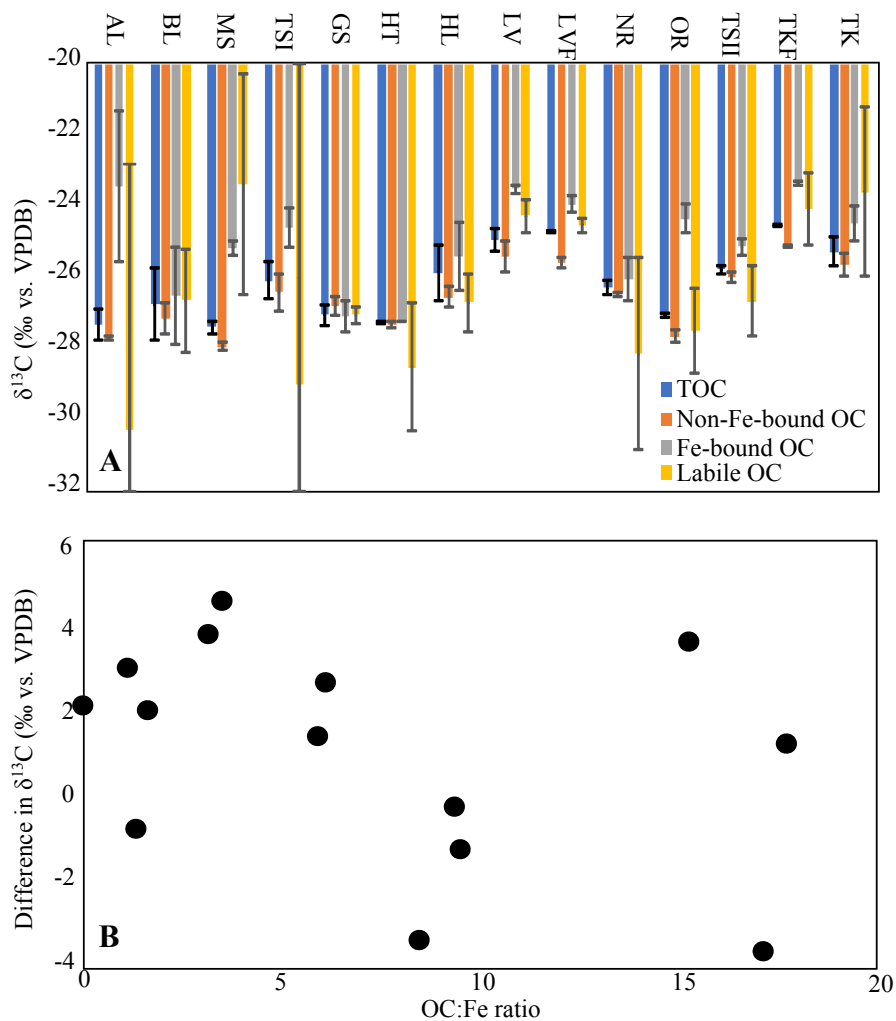
686

687

688

689

690



691

692 **Fig. 6**

693

694

695

696

697

698